ELSEVIER

Polymer 40 (1999) 3013–3023

polymer

Fluorescence study on intermolecular complex formation between mesogenic biphenyl moieties of main-chain thermotropic liquid–crystalline polyesters with 7–18 methylene units

Hsu Wen Huang[a,*], Kazuyuki Horie[a], Masatoshi Tokita[b], Junji Watanabe[b]

[a]*Department of Chemistry and Biotechnology, Graduate School of Engineering, The University of Tokyo, 7-3-1 Hongo, Bunkyo-ku, Tokyo 113-8656, Japan*
[b]*Department of Polymer Chemistry, Tokyo Institute of Technology, Ookayama, Meguro-ku, Tokyo 152-8552, Japan*

Received 27 March 1998; revised 15 May 1998; accepted 13 July 1998

Abstract

By using fluorescence spectroscopy together with d.s.c. and WAXD, structure analysis for main-chain thermotropic LC polyesters (PB-*n*), containing $n = 7–18$ methylene units, was carried out. The strong excitation-wavelength dependence of fluorescence and red shift of fluorescence peak wavelengths excited at various wavelengths during heating for all PB-*n* were found to depend on different degrees of overlap between mesogenic biphenyl moieties. The red shifts for fluorescence excited at 320 nm from room temperature to crystalline–S_H transition temperature for PB-16 (26 nm) and PB-18 (36 nm) are larger than those for PB-8 (14 nm) and PB-10 (16 nm), owing to the mobile packing structure in crystalline phase for PB-16 and PB-18 with flexible and longer spacer lengths. According to the much longer average fluorescence peak wavelengths for PB-16 (399 nm) and PB-18 (401 nm) in S_H phase than those for PB-8 (381 nm) and PB-10 (385 nm), the degree of overlap between two mesogenic biphenyl moieties in S_H phase for PB-*n* was proved to decrease and the interaction between a carbonyl group and a phenyl ring increased with its increasing methylene units. Fluorescence spectroscopy was demonstrated to be effective in proving the difference in molecular interaction between mesogenic moieties for LCP with various spacer lengths.

Keywords: Fluorescence; Liquid–crystalline polyester; Molecular interaction

1. Introduction

Mesogenic groups can be incorporated into a polymer as side chains resulting in a side-chain liquid–crystalline polymer (SLCP), or as part of the main chain resulting in a main-chain liquid–crystalline polymer (MLCP). In the SLCP case, particularly if the mesogenic group is attached through a flexible spacer, the molecular conformation is not altered by the formation of the mesophase. Thus, the polymeric and mesogenic effects are essentially uncoupled. On the other hand, in the MLCP case, the polymer molecule must form conformation and packing which are compatible with the structure of its mesophase, thus, the polymeric and mesogenic effects are closely coupled, and are often predictable from those of the low-molecular-weight mesogen group. Hence, the mesogenic moieties play an important role in determining the physical properties of MLCP.

It is well known that characteristic LC behaviour has an essential relationship with the molecular interaction between mesogenic moieties of MLCP. These MLCPs have also been attracting much attention owing to their scientific interests and numerous industrial applications [1,2]. Thus, it is important to study the molecular interaction between mesogenic moieties to elucidate the molecular level behaviour of LCP. Various fluorescent species in polymers, such as monomeric chromophores, excimers, and ground-state complexes, are demonstrated to originate in the difference in formation of molecular interaction between moieties of polymers [3–6]. Thus, the change in molecular interaction of LCPs can be studied directly by investigating the change in fluorescence behaviour of fluorescing complexes in LCPs [7–11]. Based on this concept, we studied the molecular interaction between mesogenic moieties of several thermotropic LC polyesters [7–9] and a lyotropic LCP [10]. In the fluorescence study on the intermolecular complex formation between mesogenic biphenyl moieties of a thermotropic LC polyester (PB-10) [11], a strong excitation-wavelength dependence of fluorescence was observed and proved to be due to the formation of various intermolecular ground-state complexes corresponding to

* Corresponding author.

0032-3861/99/$ - see front matter
PII: S0032-3861(98)00548-5

different degrees of overlap between biphenyl moieties. Moreover, the fluorescence peak wavelengths of these intermolecular ground-state complexes shift gradually to longer wavelengths with increasing temperature, and converge to become a structureless emission peak centred at 429 nm in isotropic phase.

In the present paper, by changing the number of methylene units of PB-*n* from $n = 7$ to 18, we continue to study the fluorescence behaviour of PB-*n* with various spacer lengths. Differential scanning calorimetry (d.s.c.) and wide-angle X-ray diffraction (WAXD) are also applied to investigate the microstructure of PB-*n*. Additionally, we compare the change in intermolecular complex formation during phase transition processes of PB-*n* with various spacer lengths.

2. Experimental

2.1. Materials

The chemical structure of the PB-*n* series thermotropic LC polyester is shown below.

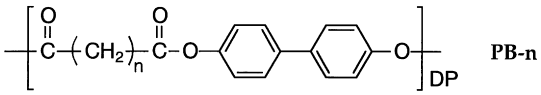

We designate these polymers by the letters PB followed by the number, *n*, of methylene units in the dicarboxylic acid. PB-*n* was prepared by melt transesterification using equimolar amounts of 4,4′-diacetoxybiphenyl and a corresponding dicarboxylic acid as reported previously [12–14]. In an effort to provide a common thermal prehistory, all the samples were placed on a quartz plate, annealed at its isotropic temperature for 10 min, and then cooled to room temperature before measurements.

2.2. Measurements

D.s.c. measurements were performed with a Perkin-Elmer DSC II differential scanning calorimeter. Samples of about 10 mg were examined at a scanning rate of 10°C/min under a flow of dry nitrogen.

WAXD measurements were carried out with a Rigaku-Denki RU-200 X-ray generator system equipped with a flat-plate camera using nickel-filtered Cu Kα radiation. The distance from the sample to the film was determined by using silicon powder. The sample temperature was controlled by a Mettler FP-80 hot stage with a FP-82 central processor.

Steady-state fluorescence spectra were measured with a Hitachi 850 fluorescence spectrophotometer equipped with a 30-kV xenon lamp. The bandpasses were 5 nm for both excitation and emission monochromators. The fluorescence and its excitation spectra were measured in a front-face arrangement to minimize the self-absorption. The temperature of the LCPs was controlled by means of an Alpha Engineering thermostat coupled with a temperature-controlling unit.

3. Results and discussion

3.1. Thermal properties of PB-n

According to previous works, PB-7 shows a crystalline (K) phase and a narrow smectic (S) phase during heating [13]. PB-8 and PB-10 show a low temperature K_1 crystalline phase and a wide and stable smectic H (S_H) phase during heating [12–16]. Moreover, an additional high temperature K_2 crystalline phase formed between K_1 and S_H phase for PB-16 and PB-18 was ascertained by d.s.c. and WAXD studies [16]. Typical examples of the second heating d.s.c. thermograms of PB-*n* with various spacer lengths are illustrated in Fig. 1. PB-7 (a) shows a complicated crystal–smectic and a sharp smectic–isotropic (I) transition around 227 and 243°C, respectively. PB-8 (b) shows a K_1–S_H and a S_H–I transition at 215 and 284°C, respectively. PB-10 (c) also shows a K_1–S_H and a S_H–I transition at 207 and 255°C, respectively. PB-16 (d) shows K_1–K_2 (177°C), K_2–S_H (188°C), and S_H–I (210°C) transition. Similarly, PB-18 (e) shows K_1–K_2 (167°C), K_2–S_H (178°C), and S_H–I (200°C) transition.

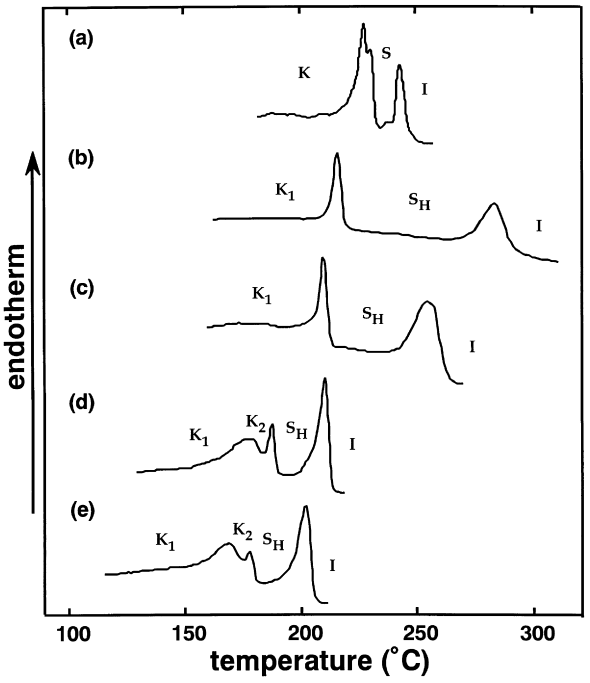

Fig. 1. The second heating DSC thermograms of: (a) PB-7; (b) PB-8; (c) PB-10; (d) PB-16; and (e) PB-18.

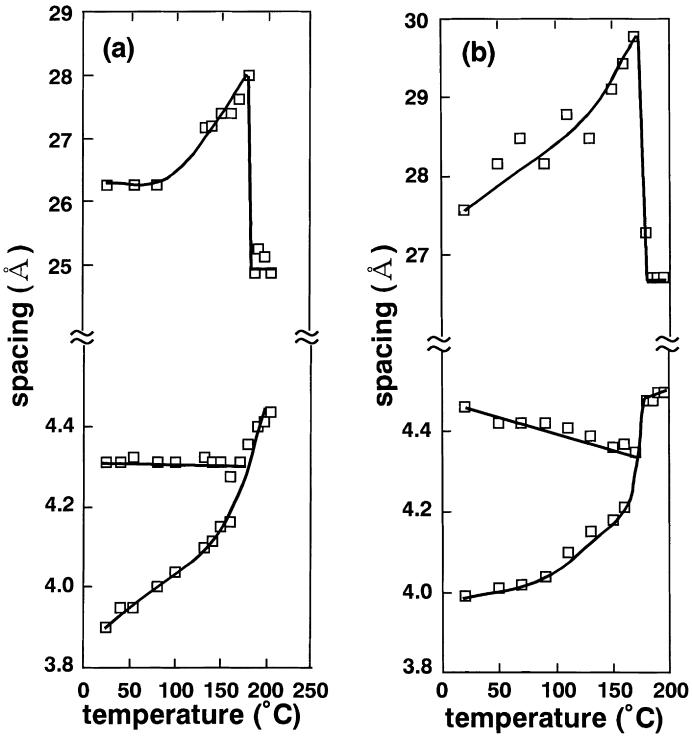

Fig. 2. Temperature dependence of some selected spacings for: (a) PB-16; and (b) PB-18.

3.2. Layer spacing change of PB-n during heating

In previous papers, we have shown that the layer spacing of PB-8 [13] and PB-10 [11] remains constantly before crystalline–S_H transition temperature, and decreases abruptly after the crystalline–S_H transition. The temperature dependence of some selected spacings for PB-16 (a) and PB-18 (b) are depicted in Fig. 2. As shown in Fig. 2a (top), the layer spacing of PB-16 increases gradually from 26.2 to 28.0 Å before crystalline–S_H transition temperature and decreases abruptly after crystalline–S_H transition. As an analogous manner, the layer spacing of PB-18 (top, Fig. 2b) also increases gradually from 27.6 to 29.8 Å before crystalline–S_H transition temperature and decreases abruptly after crystalline–S_H transition. This increase in layer spacing before crystalline–S_H transition for PB-16 and PB-18 strongly indicates the formation of an additional high temperature K_2 crystalline phase between low temperature K_1 crystalline phase and S_H phase.

3.3. Fluorescence and its excitation spectra of PB-n in crystalline phase and their excitation-wavelength dependence at room temperature

In the fluorescence study of PB-10 [11], by using biphenyl and diacetoxybiphenyl as model compounds, we concluded that the intermolecular ground-state complex of two fully overlapping biphenyl groups shows fluorescence at about 360 nm. The fluorescence at 385–422 nm of PB-10 (excited at 330–360 nm) was demonstrated to be due to the intermolecular ground-state complexes with molecular arrangements between two biphenyl moieties with less overlapping, which induce a stronger intermolecular interaction (electronic distribution change) between the ester and biphenyl moieties than those between two fully overlapping segments [11]. Moreover, the monomer fluorescence of PB-10 was confirmed to be around 340 nm [11].

Fig. 3 shows the fluorescence (right) and its excitation spectra (left) of PB-*n* in crystalline phase at room temperature. As can be seen in the fluorescence spectra excited at various excitation wavelengths, all PB-*n* show the identical monomer fluorescence around 340 nm (a). By being excited at various excitation wavelengths (b–i), all PB-*n* show various fluorescence peak wavelengths at 360–475 nm. Moreover, the shapes of fluorescence excitation spectra of PB-*n* (left) for the fluorescence at 360–475 nm (b′ and c′) disagree with those for the monomer (a′). This indicates that the fluorescence at 360–475 nm is not due to excimer or exciplex but to various intermolecular ground-state complexes. Based on these results, we conclude for PB-*n* with various spacer lengths, that this kind of excitation-wavelength dependence of intermolecular ground-state complex fluorescence is due to the aggregation structures with different degrees of overlap between biphenyl moieties.

PB-*n* with even-number methylene units ($n = 8$, 10, 16, 18) have been assumed to show identical microstructure of K_1 crystalline phase at room temperature from WAXD measurements [16]. However, according to their fluorescence spectra shown in the right part of Fig. 3(B–E), their

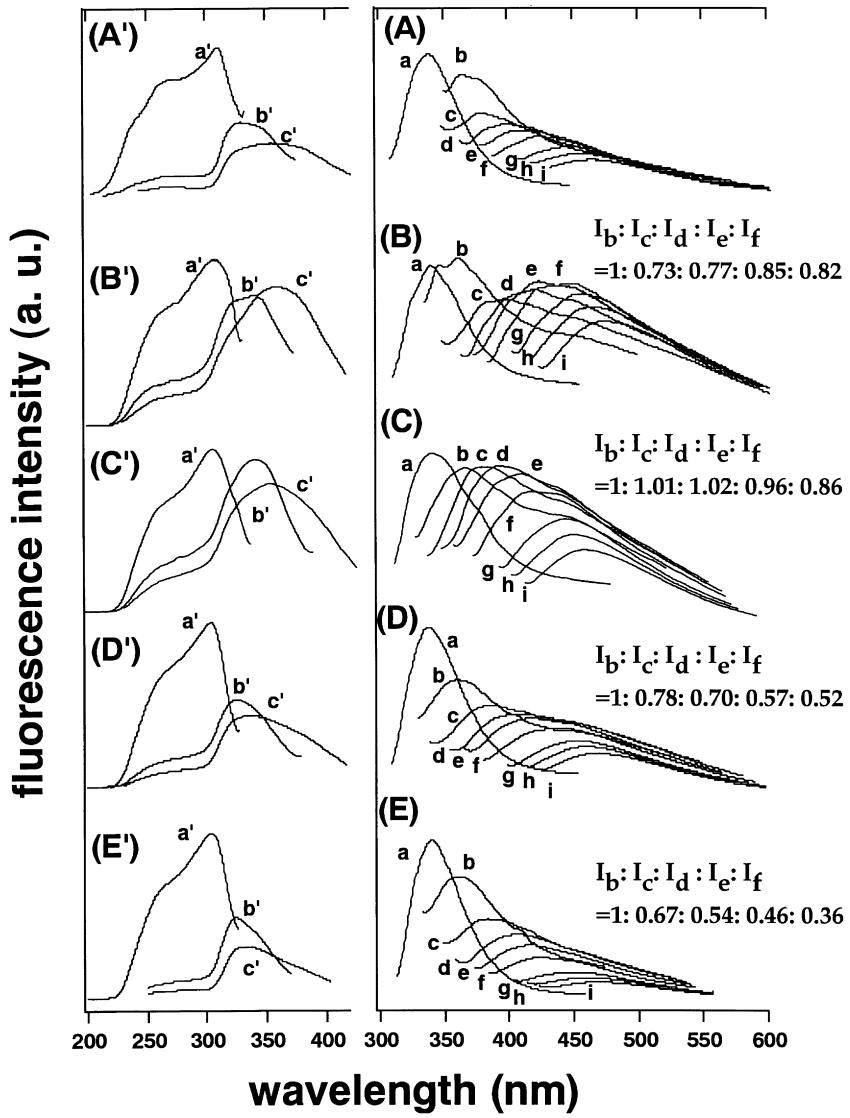

Fig. 3. Fluorescence (right) and its excitation spectra (left) for PB-7 (A,A′), PB-8 (B,B′), PB-10 (C,C′), PB-16 (D,D′), and PB-18 (E,E′) in crystalline phase at room temperature. (a–i) The fluorescence spectra excited at 300, 320, 330, 340, 350, 360, 380, 390 and 400 nm, respectively. (a′–c′) The fluorescence excitation spectra monitored at 340, 400 and 450 nm, respectively.

relative fluorescence intensity ratios (I_b:I_c:I_d:I_e:I_f) for aggregation structures originating from different degrees of overlap between biphenyl moieties for PB-8 (B), PB-10 (C), PB-16 (D) and PB-18 (E) are all different from each other. This indicates that the distribution of the aggregation structures related to the degree of overlap between two biphenyl moieties depends on their spacer lengths, though they are all in K_1 crystalline phase at room temperature.

3.4. Factors to be considered in fluorescence properties of PB-n

Although fluorescence method is an effective tool for investigating the molecular level information of polymers [3–6], there are still some factors to be considered for avoiding artifacts, especially for highly light scattered LCP samples. Since LCP is generally a turbid sample, it is inevitable to consider the factors of scattering and reabsorption. For the scattering factor, according to our previous fluorescence study of a typical LC polyester [8], non-annealed samples show violent change in scattering intensity and unreliable fluorescence spectra for analysis during phase transition, but annealed samples show stable change in scattering intensity and reliable fluorescence spectra for analysis during phase transition (Fig. 3 in Ref. [8]). This indicates that the scattering factor of PB-*n* can be avoided by annealing process as mentioned in Section 2. Moreover, in order to compare with results of other measurements, the identical thermal history of the sample is indispensable. For the reabsorption factor, fluorescence measurements are performed by a front-face arrangement to reduce the reabsorption and detect the fluorescence from the surface of the sample. However, the fluorescence excitation spectra were still distorted, but the fluorescence spectra were

reliable. Thus, the fluorescence excitation spectra are discussed only with their shape without any further interpretation.

Since LCP samples are usually in aggregated states, it is important to clarify the fluorescent species of LCP by using model compounds. In the case of PB-10 [11], by comparing the fluorescence spectra of model compounds (biphenyl and diacetoxybiphenyl) in dilute solutions and in the crystal state, monomer fluorescence of PB-10 was confirmed at about 340 nm, and the fluorescence at about 360 nm was demonstrated to be due to the intermolecular ground-state complex between two fully overlapping biphenyl groups (Fig. 3 in Ref. [11]). This implies that the biphenyl moieties interact strongly with each other to form intermolecular ground-state complexes. Additionally, the fluorescence intensity of biphenyl, diacetoxybiphenyl, and PB-10 is almost the same as each other. This indicates that the ester group does not act as a quencher in this system, but induces the change in electronic distribution to form intermolecular ground-state complexes between biphenyl and ester moieties.

Generally speaking, energy transfer from one site to another site, with dissipation of energy or energy migration among the same kind of chromorphores, should be considered in a densely packed chromophore polymer system as PB-*n*. As to the occurrence of energy transfer, since the chromophore is the only biphenyl moiety in PB-*n*, the possibility of energy transfer might be concerned with the one from excited monomer to intermolecular ground-state complex, and hence the fluorescence excitation spectra of monomer and intermolecular ground-state complexes should be almost identical. But the fluorescence excitation spectra of intermolecular ground-state complexes are different from those of monomer as shown in Fig. 3. This indicates that the factor of energy transfer is not necessary to be considered in this study. As to the occurrence of energy migration, if energy migration was a predominant factor in PB-*n*, the excitation energy of intermolecular ground-state complexes would have migrated to a similar most stable energy level, resulting in emitting fluorescence at the same wavelength, but not showing the various fluorescence peak wavelengths which depend on the change in excitation wavelength. This implies that the energy migration is not a predominant factor in PB-*n*. However, the characteristic fluorescence property of PB-*n* is the marked excitation wavelength dependence of fluorescence, therefore, it is necessary to confirm this phenomenon exactly. We studied the fluorescence behaviour of LC polyesters with mesogenic 4,4′-biphenyldicarboxylate moieties (BB-*n*) whose mesogenic moiety is different only in the sequence of oxygen in ester group comparing with PB-*n* [17]. According to the fluorescence and its excitation spectra for BB-*n* (Fig. 2 in Ref. [17]), BB-5 and BB-6 show fluorescence only at 390 nm and 384 nm, respectively, independent of excitation wavelength. Moreover, based on the WAXD studies of BB-*n* [18,19], BB-*n* show higher uniformity in molecular arrangement than that for PB-*n* crystalline phase. This ascertains that the excitation wavelength dependence of fluorescence for PB-*n* is due to the existence of various kinds of molecular packing and low uniformity in crystalline phase.

3.5. Change in fluorescence and its excitation spectra of PB-n during heating

The fluorescence spectra of PB-18 excited at various excitation wavelengths during heating are shown in the right part of Fig. 4. The wavelength of fluorescence peak excited at 320 nm (b, bold curves), which corresponds to the aggregation structure of two fully overlapping biphenyl moieties at room temperature, shifts gradually from 360 to 418 nm during heating. This is because the fully overlapping molecular arrangement at room temperature changes gradually to a partially overlapping molecular arrangement with increasing temperature, namely, the main intermolecular interaction between mesogenic moieties changes from one between two fully overlapping biphenyl groups to one between a biphenyl and an ester moiety, and alters the electronic distribution between mesogenic moieties to strengthen molecular interaction leading to a red-shifted fluorescence. Correspondingly, it is not surprising that other fluorescence wavelengths related to the various degrees of overlap between two biphenyl groups (c–f) do not shift as much as for two fully overlapping biphenyl groups (b, bold curves), owing to the molecular arrangement with an initial smaller overlap. The monomer fluorescence peak at 337 nm and emission at 448–466 nm (g–i) are observed almost invariably during heating. It is reasonable that the monomer fluorescence peak does not shift during heating considering the consistency of the electronic distribution in an independent mesogenic moiety. Unfortunately, it is difficult to confirm the origin of fluorescence at 448–466 nm (g–i), which may be due to the charge transfer interaction of highly mobile structures formed between biphenyl and ester moieties with a much lower degree of overlap. On the other hand, the fluorescence excitation spectra during heating are depicted in the left part of Fig. 4. In spite of the distortion due to monomer self-absorption and multiscattering effects, the fluorescence excitation spectra monitored at 450 nm (c′) show a broad shoulder around 390 nm during heating. This suggests that the fluorescent species at higher wavelengths become the main fluorescent species at high temperatures and that the change in fluorescence peak wavelengths is not only due to the change in the excited state but also to the change in the ground state. The change in fluorescence and its excitation spectra mentioned above are similar to the one reported for PB-10 [11]. Similarly, for other PB-*n* with even-number methylene units ($n = 8, 16$), the changes in their fluorescence and its excitation spectra are also similar to the one for PB-18.

Fig. 5 shows the fluorescence (right) and its excitation

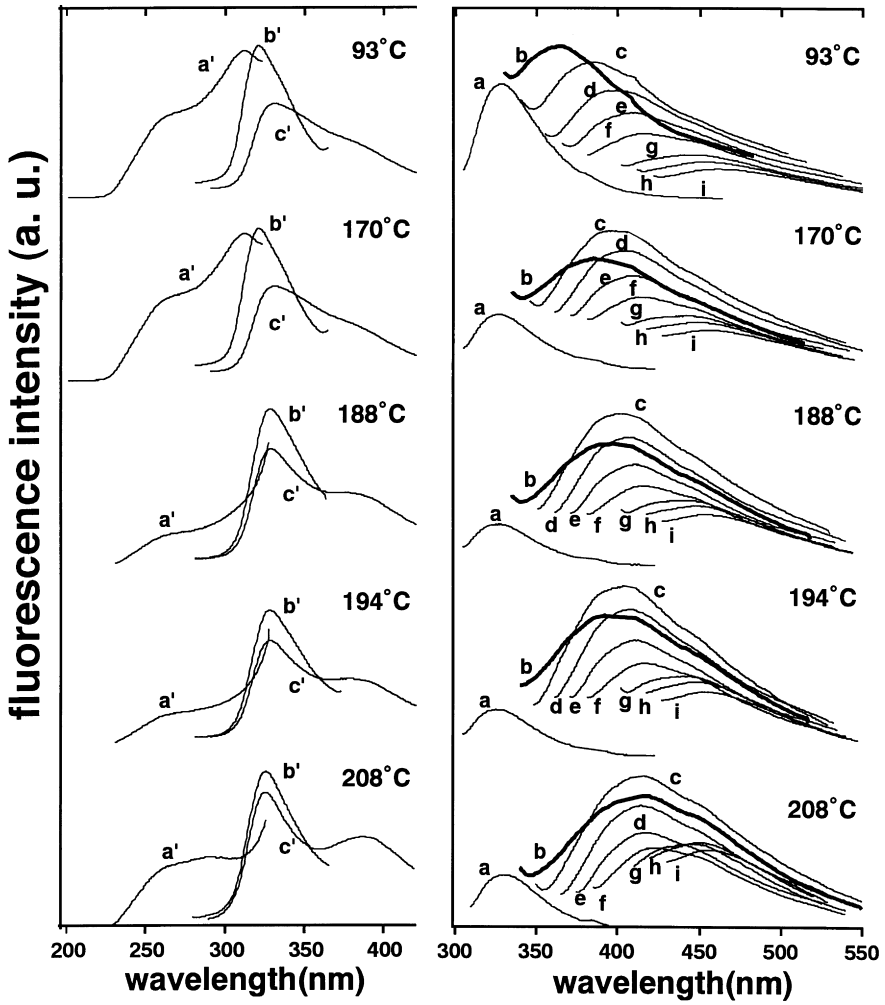

Fig. 4. Fluorescence (right) and its excitation spectra (left) of PB-18 during heating. (a–i) The fluorescence spectra excited at 300, 320, 330, 340, 350, 360, 380, 390 and 400 nm, respectively. (a′–c′) The fluorescence excitation spectra monitored at 340, 400 and 450 nm, respectively.

spectra (left) of PB-7 during heating. As can be seen in the fluorescence spectra (right), the fluorescence peak wavelengths related to various degrees of overlap between two biphenyl moieties (b–f) show red-shifted fluorescence during heating. Moreover, although the fluorescence excitation spectra at high temperatures (233 and 248°C) are distorted, fluorescence excitation spectra monitored at 450 nm (c′) under 195°C also show a broad shoulder around 390 nm. These changes in fluorescence and its excitation spectra are almost in accord with those changes for PB-*n* with even-number methylene units. Consequently, independent of PB-*n* with odd- or even-number methylene units, we conclude that the molecular interaction between mesogenic moieties of all PB-*n* change from the one between two fully overlapping biphenyl groups to the one between a biphenyl and an ester moiety during heating.

Fig. 6 shows the fluorescence (right) and its excitation spectra (left) of PB-*n* in isotropic phase. As can be seen in their fluorescence spectra (right), except for the monomer fluorescence (a) and fluorescence at 445–475 nm (g–i), fluorescence excited at 320–360 nm (b–f) show only a broad structureless band around 415–430 nm, in contrast to the fact that these fluorescent species show strong excitation wavelength dependence in crystalline and S_H phase. Independent of PB-*n* with odd- or even-number methylene units, we conclude that all PB-*n* show only one kind of identical steady-state molecular interaction between biphenyl moieties in the isotropic phase. This is reasonable because the mobile surroundings around chromophores in isotropic phase of PB-*n* have no correlation to the spacer length.

3.6. Comparison of the change in fluorescence peak wavelength for PB-n during heating

The changes in fluorescence peak wavelengths excited at various excitation wavelengths during heating for PB-*n* with even-number methylene units are plotted in Fig. 7. For PB-8 (a), the peak wavelength change for fluorescence excited at 320 nm (♦) is the largest one. This is reasonable since two fully overlapping biphenyl groups at room temperature change interaction structure most clearly during heating.

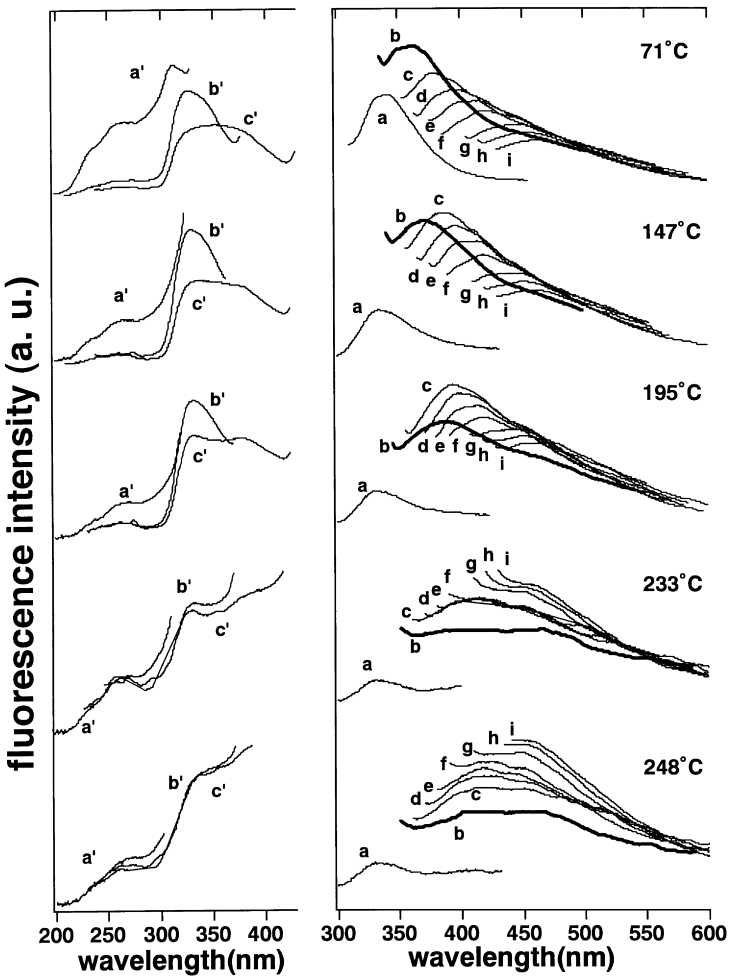

Fig. 5. Fluorescence (right) and its excitation spectra (left) of PB-7 during heating. (a–i) The fluorescence spectra excited at 300, 320, 330, 340, 350, 360, 380, 390 and 400 nm, respectively. (a′–c′) The fluorescence excitation spectra monitored at 340, 400 and 450 nm, respectively.

The plot shows two breaks at 158 and 283°C; the temperature dependence of the molecular interaction changes first at 158°C, a temperature significantly lower than the K_1–S_H transition temperature measured by d.s.c. and WAXD (215°C). This implies that the temperature effect initially makes the phase transition start in a local microstructure level (molecular interaction between mesogenic moieties), and then it extends to the macrostructure change (the entire phase transition). The temperature dependence of the change in molecular interaction changes again at 283°C, which is near the S_H-isotropic transition temperature (284°C). Thus, this indicates that the temperature dependence of the change in molecular interaction for various phases are different. This kind of change in temperature dependence of fluorescence peak wavelengths was also reported for PB-10 [11] as shown in Fig. 7b. Similarly, for PB-*n* with longer spacer lengths, temperature dependence of fluorescence excited at 320 nm (♦) of PB-16 (c) shows a first break at 163°C, a temperature lower than the K_1–K_2 transition temperature detected by d.s.c. and WAXD (177°C), and second break around 206°C, which is near the S_H–I transition temperature (210°C). According to Fig. 7d, PB-18 also shows similar change in temperature dependence of fluorescence excited at 320 nm (♦) as PB-16, namely, two breaks at 147 and 203°C. This suggests that PB-*n* with longer spacer lengths (PB-16 and PB-18) also show microscopic pretransition before K_1–K_2 transition temperature as the microscopic pretransition before K_1–S_H transition temperature for PB-8 and PB-10. Unfortunately, temperature dependence of fluorescence peak wavelengths for PB-16 and PB-18 does not show a break at around the K_2–S_H transition temperature. However, by comparing the difference of red-shift wavelength for fluorescence excited at 320 nm (♦) at room temperature with that at crystalline–S_H transition temperature for PB-*n*, fluorescence peak wavelengths of PB-8 and PB-10 shift about 14 and 16 nm (shadow area), respectively; on the contrary, the amounts of red shifts for PB-16 and PB-18 (shadow area) are about 26 and 36 nm, respectively. This indicates that the degrees of overlap between two biphenyl moieties of PB-16 and PB-18 decrease much more before crystalline–S_H transition than PB-8 and PB-10 do, which is due to the flexible and longer spacer lengths to make the molecular packing become more mobile. This kind of increase in the amounts

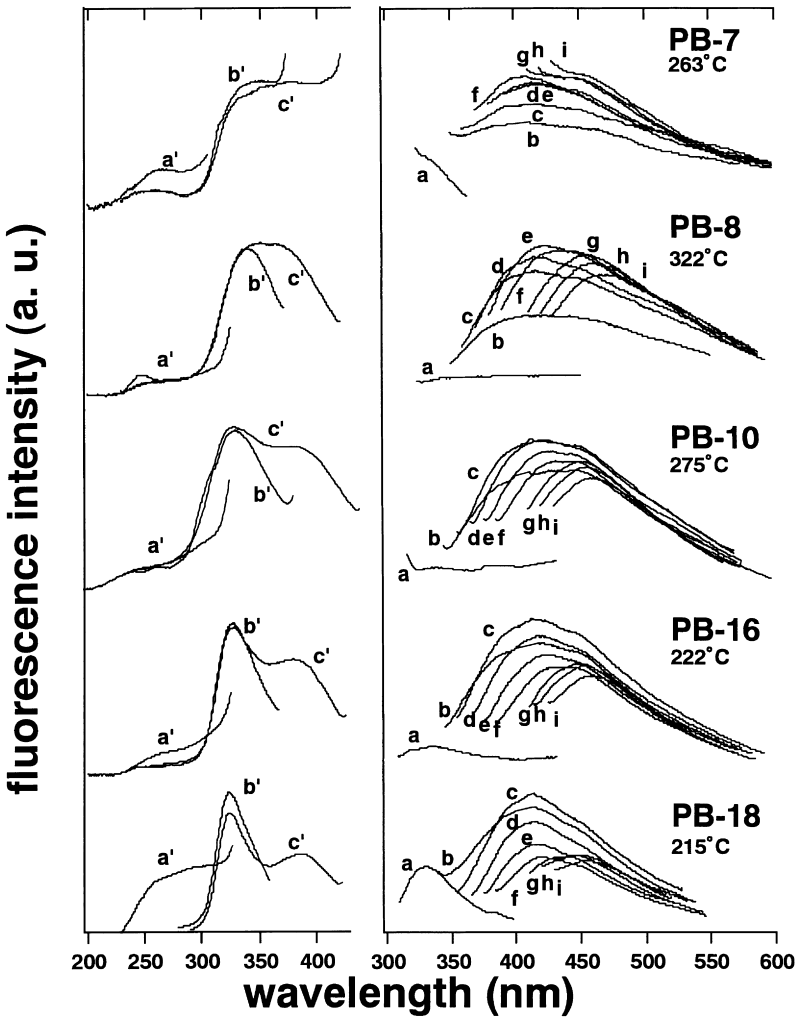

Fig. 6. Fluorescence (right) and its excitation spectra (left) of PB-*n* in isotropic phase. (a–i) The fluorescence spectra excited at 300, 320, 330, 340, 350, 360, 380, 390 and 400 nm, respectively. (a′–c′) The fluorescence excitation spectra monitored at 340, 400 and 450 nm, respectively.

of red shifts (shadow area) for PB-16 and PB-18 is in good agreement with the increase in their layer spacing before crystalline–S_H transition temperature as mentioned in the WAXD part. This also reflects the formation of a high temperature K_2 crystalline phase between low temperature K_1 crystalline phase and S_H phase for PB-16 and PB-18.

In order to compare the degree of overlap between mesogenic biphenyl moieties in S_H phase for PB-*n* with various spacer lengths, we present the change in fluorescence peak wavelength excited at 320 nm (λ_f) and the average λ_f in S_H phase as shown in the upper part of Fig. 7. PB-8 and PB-10 show average λ_f around 381 and 385 nm, respectively. But PB-16 and PB-18 show average λ_f around 399 and 401 nm, respectively. This implies that the degree of overlap between two biphenyl moieties in S_H phase of PB-*n* decreases with its increasing methylene units as shown in the illustration of tentative molecular arrangements between two mesogenic biphenyl moieties for PB-*n* (upper part of Fig. 7).

Based on the above WAXD and fluorescence results, we propose the approximate molecular arrangements between mesogenic moieties of PB-18 as an example in various phases as illustrated in Fig. 8. Since K_1 phase shows λ_f (fluorescence peak wavelength excited at 320 nm) around 360 nm corresponding to the fluorescence from two fully overlapping biphenyl groups [11], the molecular arrangement between mesogenic moieties of K_1 phase is depicted to be a fully overlapping arrangement between two biphenyl moieties (left), which is similar to the approximate molecular arrangement of crystalline phase reported for PB-8 [13]. The layer spacing increases for K_2 phase (Fig. 2b) probably owing to the extension of methylenic spacer. But λ_f shows a longer fluorescence peak wavelength than the one in K_1 phase, which is due to the change in electronic distribution between a biphenyl moiety and an ester moiety. This indicates that the degree of overlap between two biphenyl moieties in K_2 phase is lower than the one in K_1 phase. Thus, we propose the approximate molecular arrangement between mesogenic moieties of K_2 phase in the middle part of Fig. 8, which exhibits a partially overlapping molecular arrangement between two biphenyl moieties but not a fully overlapping one. For S_H phase, its

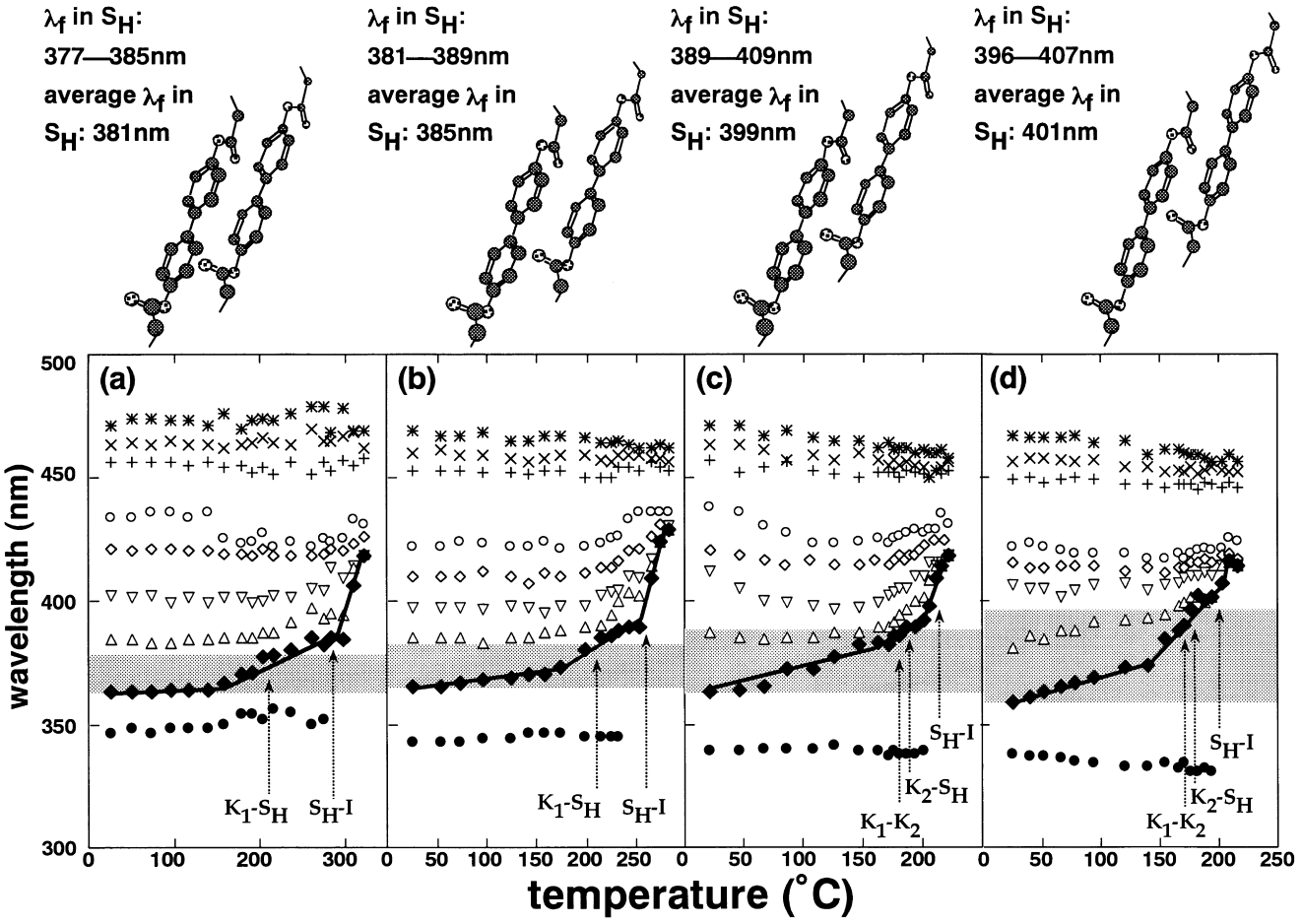

Fig. 7. Temperature dependence of the fluorescence peak wavelengths excited at various excitation wavelengths for: (a) PB-8; (b, from Ref. [11]) PB-10; (c) PB-15; and (d) PB-18, during heating. The various excitation wavelengths are as follows: (●) 300 nm; (♦) 320 nm; (△) 330 nm; (▽) 340 nm, (◇) 350 nm; (○) 360 nm; (+) 380 nm; (×) 390 nm; (*) 400 nm.

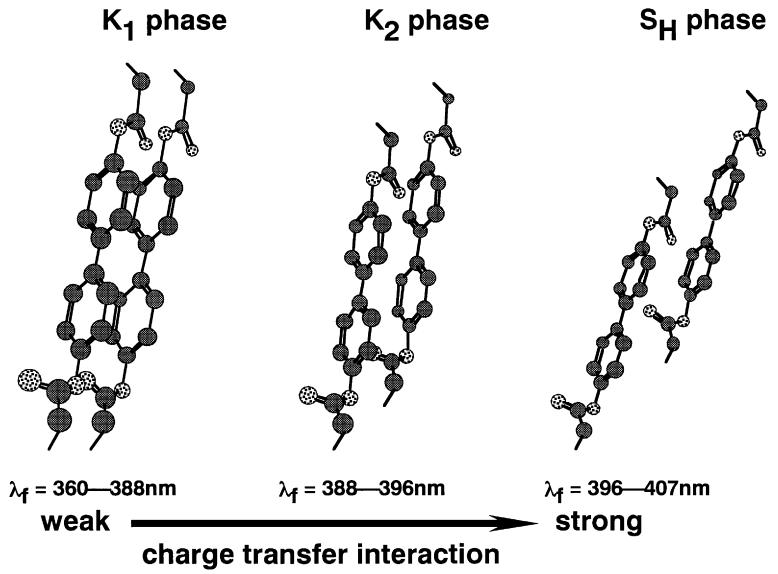

Fig. 8. Approximate molecular arrangements between mesogenic biphenyl moieties of PB-18 in various phases.

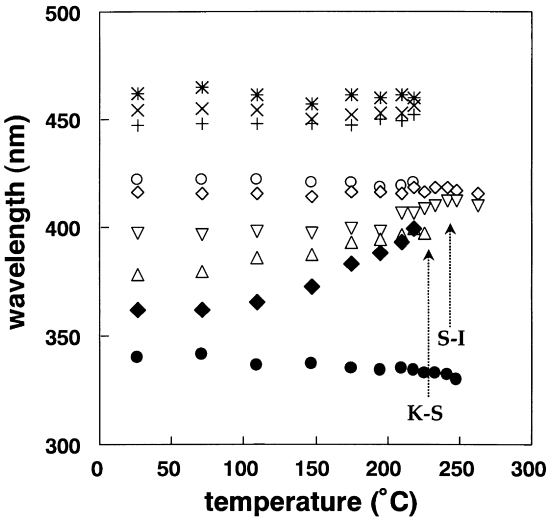

Fig. 9. Temperature dependence of the fluorescence peak wavelengths excited at various excitation wavelengths during heating for PB-7. The various excitation wavelengths are as follows: (●) 300 nm; (◆) 320 nm; (△) 330 nm; (▽) 340 nm; (◇) 350 nm; (○) 360 nm; (+) 380 nm; (×) 390 nm; (*) 400 nm.

layer spacing decreases abruptly and λ_f shows much longer fluorescence peak wavelength than those in K_1 and K_2 phase. Therefore, the approximate molecular arrangement between mesogenic moieties of S_H phase exhibits a molecular arrangement between two biphenyl moieties with a much lower degree of overlap than those in K_1 and K_2 phase as in the right part of Fig. 8, which is similar to the approximate molecular arrangement of S_H phase suggested for PB-8 [13].

Fig. 9 shows the temperature dependence of the fluorescence peak wavelengths excited at various excitation wavelengths for PB-7 during heating. Since the spectra above crystalline–smectic transition temperature (227°C) become a broad structureless band owing to the strong light scattering effect, it is difficult to determine the peak wavelength of the spectra at high temperatures. However, the fluorescence related to the degrees of overlap between two biphenyl moieties (excited at 320–360 nm) converge to a certain wavelength and the peak wavelength for fluorescence excited at 320 nm (◆) shows a red shift during heating. This indicates that the degree of overlap between two biphenyl moieties of PB-7 decreases gradually during

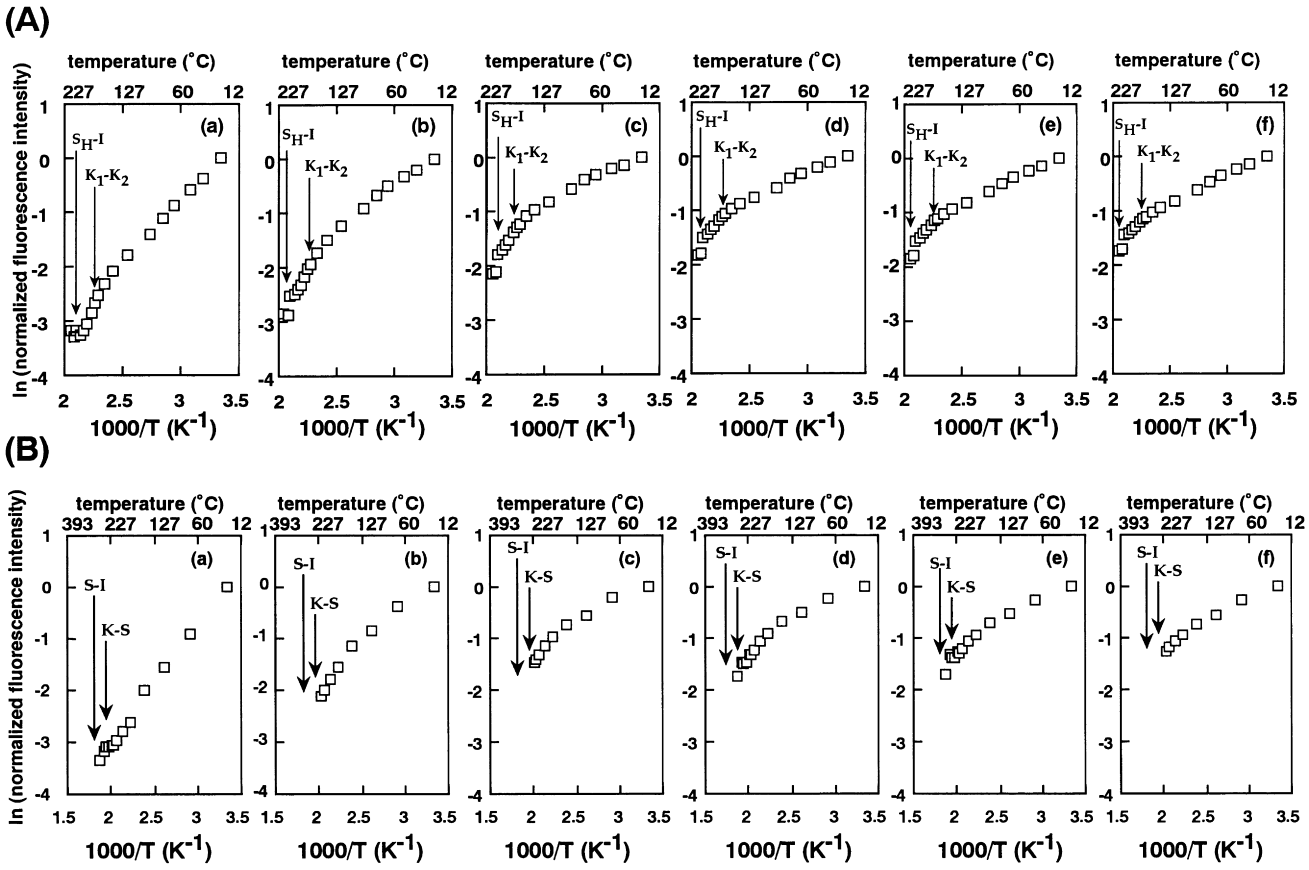

Fig. 10. Arrhenius-type plots for the change in fluorescence intensity of monomer and various intermolecular ground-state complexes during heating for PB-18 (A) and PB-7 (B). (A) The fluorescence and excitation wavelengths for monomer and various intermolecular ground-state complexes of PB-18 are as follows: (a) 338 nm (excited at 300 nm); (b) 360 nm (excited at 320 nm) (c): 381 nm (excited at 330 nm); (d) 406 nm (excited at 340 nm); (e) 416 nm (excited at 350 nm); (f) 422 nm (excited at 360 nm). (B) The fluorescence and excitation wavelengths for monomer and various intermolecular ground-state complexes of PB-7 are as follows: (a) 340 nm (excited at 300 nm); (b) 362 nm (excited at 320 nm); (c) 378 nm (excited at 330 nm); (d) 397 nm (excited at 340 nm); (e) 415 nm (excited at 350 nm); (f) 422 nm (excited at 360 nm).

heating as PB-*n* with even-number methylene units, although the LC phase of PB-7 is smectic phase.

3.7. Change in fluorescence intensity for PB-n during heating

In order to investigate the deactivation processes of monomer and various intermolecular ground-state complexes during heating, the Arrhenius-type plots for the change in fluorescence intensity during heating for PB-18 (A) and PB-7 (B) are depicted in Fig. 10. For PB-18 (A), the fluorescence intensity decreases with increasing temperature owing to the increase in radiationless transition, showing two breaks at 147 and 203°C in accordance with the change in peak wavelength of fluorescence excited at 320 nm shown in Fig. 7d. In an analogous manner, the Arrhenius-type plots for the change in fluorescence intensity during heating for PB-8 and PB-16 both show breaks around phase transition temperatures. This suggests that the deactivation processes of fluorescent species are different in various phases, which is also similar to the change in fluorescence intensity reported for PB-10 [11]. However, the temperature dependence of fluorescence intensity is affected by both the activation energy for radiationless transition and the change in the number of various fluorescent species. For PB-*n* with odd-number methylene units, Fig. 10B shows the Arrhenius-type plots for the change in fluorescence intensity during heating for PB-7. Unfortunately, it is difficult to demonstrate the whole change in fluorescence intensity of PB-7 during heating, which may be due to the interference of strong light scattering effect at high temperatures.

4. Conclusions

Based on the discovery of excitation-wavelength dependence of fluorescence for PB-10 [11], we continued to study the change in molecular interaction between mesogenic moieties for PB-*n* ($n = 7–18$) by fluorescence measurements together with d.s.c. and WAXD. As in our previous papers [7–11], d.s.c. and WAXD were used for examining the thermal properties and layer spacing change, respectively. Independent of the odd- or even-number methylene units of PB-*n*, excitation-wavelength dependence of fluorescence and red-shifting phenomenon during heating for fluorescence peak wavelengths excited at various wavelengths were ascertained for all PB-*n*. The PB-*n* with longer spacer lengths (PB-16 and PB-18) show larger red shifts in wavelength for fluorescence excited at 320 nm from room temperature to crystalline–S_H transition temperature than those for PB-*n* with shorter spacer lengths (PB-8 and PB-10), which is due to the mobile packing structure of PB-16 and PB-18 with more flexible and longer spacer lengths. The degree of overlap between two biphenyl moieties in S_H phase for various PB-*n* was confirmed to decrease with its increasing methylene units, based on the much longer average fluorescence peak wavelengths of PB-16 and PB-18 in S_H phase than those for PB-8 and PB-10. Moreover, the approximate molecular arrangement between mesogenic moieties of K_2 phase for PB-18 was proposed to be in a partially overlapping arrangement between two biphenyl moieties but not a fully overlapping one according to the red-shifting fluorescence during heating.

Acknowledgements

H.W.H. is greatly indebted to the JSPS Research Fellowship for Young Scientists for supporting his research and Ph.D. study in the University of Tokyo.

References

[1] Ciferri A, Krigbaum WR, Meyer RB, editors. Polymer liquid crystals New York: Academic Press, 1982.
[2] Isayev AI, Kyu T, Cheng SZD, editors. Liquid–crystalline polymer systems: technological advances. ACS Symposium Series No 632. Washington, DC: ACS, 1996.
[3] Lakowicz JR. Principles of fluorescence spectroscopy. New York: Plenum Press, 1986.
[4] Winnik MA, editor. Photophysical and photochemical tools in polymer science (conformation, dynamics, morphology). NATO ASI Series Dordrecht: Reidel, 1986.
[5] Itagaki H, Horie K, Mita I. Prog Polym Sci 1990;15:361.
[6] Huang HW, Horie K. Trends Polym Sci 1997;5:407.
[7] Sone M, Harkness BR, Watanabe J, Yamashita T, Horie K. Polym J 1993;25:997.
[8] Huang HW, Horie K, Yamashita T. J Polym Sci, Polym Phys Ed 1995;33:1673.
[9] Horie K, Huang HW. Macromol Symp 1997;118:229.
[10] Takahashi H, Horie K, Yamashita T, Machida S, Hannah DTB, Sherrington DC. Macromol Chem Phys 1996;197:2703.
[11] Huang HW, Horie K, Yamashita T, Machida S, Sone M, Tokita M, Watanabe J, Maeda Y. Macromolecules 1996;29:3485.
[12] Asrar J, Toriumi H, Watanabe J, Ciferri A. J Polym Sci, Polym Phys Ed 1983;21:1119.
[13] Krigbaum WR, Watanabe J, Ishikawa T. Macromolecules 1983;16:1271.
[14] Watanabe J, Krigbaum WR. Macromolecules 1984;17:2288.
[15] Maeda Y, Watanabe J. Macromolecules 1995;28:1661.
[16] Maeda Y, Mabuchi T, Watanabe J. Thermochim Acta 1995;266:189.
[17] Huang HW, Horie K, Tokita M, Watanabe J. Macromol Chem Phys (in press).
[18] Watanabe J, Hayashi M. Macromolecules 1988;21:278.
[19] Watanabe J, Hayashi M. Macromolecules 1989;22:4083.